AUTOMATIC GENERATION OF SIMPLE PARAMETRIC MODELS FOR ELECTRONIC DEVICES

Florence E. Olympie* and Randall L. Geiger**

* Departement of Electrical Engineering
Texas A&M University
College Station, TX 77843 USA

** Departement of Electrical Engineering
and Computer Engineering
Iowa State University
Ames, IA 50011 USA

Abstract:
A high-level software tool for automatic generation of simple, accurate and mathematically tractable parametric device models for arbitrarily complex physical models of electronic devices is described. For the set of equations defining the SPICE Level2 MOSFET large signal model the problem of approximating the complex and accurate closed-form formulas by simple and self-consistent polynomial expressions is addressed. The tradeoff between simplicity and accuracy will also be discussed.

I. INTRODUCTION

Circuit simulation programs such as SPICE provide complex nonlinear closed-form equations involving large sets of model parameters to describe accurately the performance of electronic devices. The complexity of those elaborate models also makes them totally untractable for analytical manipulation and inappropriate for the circuit designer to develop any intuitive understanding of the device electrical behavior. The emergence of complicated and accurate device models is causing a divergence between these models and the simple analytical models used by designers for conceptualization and optimization during the design process. This paper focuses on the development of a high-level software tool for automatic generation of simple, accurate and mathematically tractable parametric device models from arbitrarily complex physical models of electronic devices. This computer tool will be used for developing multi-dimensional approximated models of the analytical Level2 MOSFET model implemented in SPICE.

II. MOSFET DEVICE MODELS

The Level2 MOSFET model implemented in SPICE is characterized by 42 parameters and described by a large set of complex simultaneous nonlinear equations. It is an analytical one-dimensional model which includes important second order effects: channel length modulation, body effect, mobility reduction and short-channel and narrow-channel effects. The second order effects for small geometry devices involve the surface mobility reduction due to carrier-velocity saturation, the threshold voltage dependence upon the channel length and the channel width, the depletion charge sharing by the drain and the source.

Let consider the drain current as it is introduced in the Meyer's Level2 SPICE model to illustrate the complexity of the MOSFET device model:

$$I_{DS} = \frac{K_2' W}{L_{eff}} \cdot \left[(V_{GSQ} - V_{TH}^* - \frac{\eta}{2} \cdot V_{DSAT}) \cdot V_{DSAT} - \frac{2}{3}\gamma_s \left((V_{DSAT} - V_{BSQ} + \phi)^{\frac{3}{2}} - (\phi - V_{BSQ})^{\frac{3}{2}} \right) \right]$$

where the main parameters involved are defined below:

* Transconductance parameter: $K_2' = K' \cdot \frac{\mu_s}{\mu_0}$

  where $K' = \mu_0 C_{ox}$

* Effective mobility: $\mu_s = \mu_0 \left[\frac{UCRIT \epsilon_{Si}}{C_{ox}(V_{GSQ} - V_{TH})} \right]^{UEXP}$

* Threshold voltage:

$$V_{TH} = V_{TO} + \gamma \left[(\phi - V_{BSQ})^{\frac{1}{2}} - \phi^{\frac{1}{2}} \right] - \gamma\alpha(\phi - V_{BSQ})^{\frac{1}{2}} + (\phi - V_{BSQ}) \cdot \frac{\pi}{4} \cdot \frac{\epsilon_{Si}}{C_{ox} W} \delta$$

* Device width: W

* Adjusted device length: $L_{adj} = L - 2L_D$

* Effective device length: $L_{eff} = L_{adj}(1 - \lambda V_{DSQ})$

* Saturation voltage: V_{DSAT}

* Bulk threshold parameter: $\gamma_s = \gamma(1 - \alpha)$

  where

$$\alpha = \frac{1}{2} \cdot \frac{X_J}{L_{adj}} \left[\left(1 + 2\frac{W_S}{X_J}\right)^{\frac{1}{2}} + \left(1 + 2\frac{W_D}{X_J}\right)^{\frac{1}{2}} - 2 \right]$$

$$W_S = X_D(\phi - V_{BSQ})^{\frac{1}{2}}$$

$$W_D = X_D(\phi - V_{BSQ} + V_{DSQ})^{\frac{1}{2}}$$

The model also introduces various expressions for the saturation voltage V_{DSAT} and the channel length modulation parameter λ depending on the presence or the absence of the channel length modulation parameter and the speed limit of the carriers V_{MAX} in the .MODEL card specified in the SPICE input deck.

* If λ is not input and V_{MAX} is input in the .MODEL card,

$$\lambda = \frac{X_D}{L_{adj} V_{DSQ}} \cdot \left\{ \left[\frac{V_{MAX}^2 X_D^2}{4\mu_s^2} + V_{DSQ} - V_{DSAT} \right]^{\frac{1}{2}} - \frac{V_{MAX} X_D}{2\mu_s} \right\}$$

$$X_D = \sqrt{\frac{2\epsilon_s}{qN_A N_{eff}}}$$

* If λ is not input and V_{MAX} is not input in the .MODEL card,

$$\lambda = \frac{X_D}{L_{adj} V_{DSQ}} \cdot \left[\frac{V_{DSQ} - V_{DSAT}}{4} + \left(1 + \left(\frac{V_{DSQ} - V_{DSAT}}{4} \right)^2 \right)^{\frac{1}{2}} \right]^{\frac{1}{2}}$$

where

$$X_D = \sqrt{\frac{2\epsilon_s}{qN_A}}$$

* If V_{MAX} is input, then the saturation voltage is the solution of a 4th order polynomial according to the Baum and Beneking theory.

* If V_{MAX} is not input,

$$\begin{aligned} V_{DSAT} &= \frac{V_{GSQ} - V_{TH}^{*}}{\eta} \\ &+ \frac{1}{2} \left(\frac{\gamma_s}{\eta} \right)^2 \left\{ 1 - \left[1 + 4 \left(\frac{\eta}{\gamma_s} \right)^2 \left(\frac{V_{GSQ} - V_{TH}^{*}}{\eta} + \phi - V_{BSQ} \right) \right]^{\frac{1}{2}} \right\} \end{aligned}$$

* $V_{TH^*} = V_{TO} - \gamma \phi^{\frac{1}{2}} + (\phi - V_{BSQ}) \cdot \frac{\pi}{4} \cdot \frac{\epsilon_{Si}}{C_{ox} W} \delta$

Considering now the small-signal model, the small-signal output conductance g_o in the saturation region is derived by partial differentiation of the drain current with respect to the drain-to-source voltage.

$$g_o = \left. \frac{\partial I_D}{\partial V_{DS}} \right|_{Q-point}$$

The small-signal model provided in SPICE for the output conductance was developed by making major simplicity assumptions to the device model and therefore implemented as a unique expression for this small-signal parameter. It is defined as follows:

$$\begin{aligned} g_o &= \frac{\lambda}{1 - \lambda V_{DS}} \cdot I_{DS} \\ &+ \frac{\gamma}{6} \cdot \frac{X_D}{L_{adj}} \cdot \frac{K_2' W}{L_{adj}} (\phi + V_{DS} - V_{BS})^{-\frac{1}{2}} \left(1 + 2 \frac{W_D}{X_D} \right)^{-\frac{1}{2}} \end{aligned}$$

$$\cdot\left[(V_{DSAT}-V_{BS}+\phi)^{\frac{3}{2}}-(\phi-V_{BS})^{\frac{3}{2}}\right]$$

Nevertheless, hand-calculations of the output conductance determined four sub-models within the Level2 model according to the major role played by both parameters λ and V_{MAX}. Mathematical computations carried out in order to obtain the exact closed-form expression of the output conductance in each case led to the following equations:

* Case 1: λ input, V_{MAX} not input:

$$\begin{aligned} g_o &= \frac{\lambda}{1-\lambda V_{DS}}\cdot I_{DS} \\ &+ \frac{\gamma}{6}\cdot\frac{X_D}{L_{adj}}\cdot\frac{K_2'W}{L_{eff}}(\phi+V_{DS}-V_{BS})^{-\frac{1}{2}}\left(1+2\frac{W_D}{X_J}\right)^{-\frac{1}{2}} \\ &\cdot\left[(V_{DSAT}-V_{BS}+\phi)^{\frac{3}{2}}-(\phi-V_{BS})^{\frac{3}{2}}\right] \\ &- \frac{\gamma}{4}\cdot\frac{X_D}{L_{adj}}\cdot\frac{UEXP}{V_{GS}-V_{TH}}(\phi-V_{BS})^{\frac{1}{2}}\left(1+2\frac{W_D}{X_J}\right)^{-\frac{1}{2}}(\phi-V_{BS}+V_{DS})^{-\frac{1}{2}}I_{DS} \\ &+ \frac{K_2'W}{L_{eff}}\left[(V_{GS}-V_{TH}^*-\eta V_{DSAT})-\gamma_s(V_{DSAT}-V_{BS}+\phi)^{\frac{1}{2}}\right]\frac{\partial V_{DSAT}}{\partial V_{DS}} \end{aligned}$$

where

$$\begin{aligned} \frac{\partial V_{DSAT}}{\partial V_{DS}} &= -\frac{1}{4}\cdot\frac{\gamma_s}{\eta}\cdot\frac{\gamma}{\eta}\cdot\frac{X_D}{L_{adj}}\cdot\left(1+2\frac{W_D}{X_J}\right)^{-\frac{1}{2}}(\phi-V_{BS}+V_{DS})^{-\frac{1}{2}} \\ &\cdot\left\{1-\left[1+4\left(\frac{\eta}{\gamma_s}\right)^2\left(\frac{V_{GS}-V_{TH}^*}{\eta}+\phi-V_{BS}\right)\right]^{\frac{1}{2}}\right\} \\ &- \frac{1}{2}\cdot\frac{\gamma}{\gamma_s}\cdot\frac{X_D}{L_{adj}}\left(1+2\frac{W_D}{X_J}\right)^{-\frac{1}{2}}(\phi-V_{BS}+V_{DS})^{-\frac{1}{2}} \\ &\cdot\left[1+4\left(\frac{\eta}{\gamma_s}\right)^2\left(\frac{V_{GS}-V_{TH}^*}{\eta}+\phi-V_{BS}\right)\right]^{-\frac{1}{2}} \\ &\cdot\left(\frac{V_{GS}-V_{TH}^*}{\eta}+\phi-V_{BS}\right) \end{aligned}$$

* Case 2: λ input, V_{MAX} input:

$$\begin{aligned} g_o &= \frac{\lambda}{1-\lambda V_{DS}}\cdot I_{DS} \\ &+ \frac{\gamma}{6}\cdot\frac{X_D}{L_{adj}}\cdot\frac{K_2'W}{L_{eff}}(\phi+V_{DS}-V_{BS})^{-\frac{1}{2}}\left(1+2\frac{W_D}{X_J}\right)^{-\frac{1}{2}} \end{aligned}$$

$$
\begin{aligned}
&\cdot\left[(V_{DSAT}-V_{BS}+\phi)^{\frac{3}{2}}-(\phi-V_{BS})^{\frac{3}{2}}\right] \\
-&\;\frac{\gamma}{4}\cdot\frac{X_D}{L_{adj}}\cdot\frac{UEXP}{V_{GS}-V_{TH}}(\phi-V_{BS})^{\frac{1}{2}}\left(1+2\frac{W_D}{X_J}\right)^{-\frac{1}{2}}(\phi-V_{BS}+V_{DS})^{-\frac{1}{2}}I_{DS} \\
+&\;\frac{K_2'W}{L_{eff}}\left[(V_{GS}-V_{TH}^{*}-\eta V_{DSAT})-\gamma_s(V_{DSAT}-V_{BS}+\phi)^{\frac{1}{2}}\right]\frac{\partial V_{DSAT}}{\partial V_{DS}}
\end{aligned}
$$

where the saturation voltage is solution of a 4^{th} order polynomial according to Baum's theory of scattering velocity saturation. The SPICE source code evaluates the saturation voltage by solving the 4^{th} order polynomial through an iterative algorithm. This algorithm was extended to implement the partial derivative of the saturation voltage.

* Case 3: λ not input, V_{MAX} not input:

$$
\begin{aligned}
g_o \;=\;& -\frac{\gamma}{4}\cdot\frac{X_D}{L_{adj}}\cdot\frac{UEXP}{V_{GS}-V_{TH}}(\phi-V_{BS})^{\frac{1}{2}}\left(1+2\frac{W_D}{X_J}\right)^{-\frac{1}{2}}(\phi-V_{BS}+V_{DS})^{-\frac{1}{2}}I_{DS} \\
&+\frac{1}{8}\cdot\frac{X_D}{L_{adj}}\left[\frac{V_{DS}-V_{DSAT}}{4}+\left(1+\left(\frac{V_{DS}-V_{DSAT}}{4}\right)^2\right)^{\frac{1}{2}}\right]^{-\frac{1}{2}} \\
&\cdot\left[1+\left(\frac{V_{DS}-V_{DSAT}}{4}\right)\left(1+\left(\frac{V_{DS}-V_{DSAT}}{4}\right)^2\right)^{-\frac{1}{2}}\right]\left(1-\frac{\partial V_{DSAT}}{\partial V_{DS}}\right)\frac{I_{DS}}{1-\lambda V_{DS}} \\
&+\frac{K_2'W}{L_{eff}}\left[V_{GS}-V_{TH}^{*}-\eta V_{DSAT}-\gamma_s(V_{DSAT}-V_{BS}+\phi)^{\frac{1}{2}}\right]\frac{\partial V_{DSAT}}{\partial V_{DS}} \\
&+\frac{\gamma}{6}\cdot\frac{X_D}{L_{adj}}\cdot\frac{K_2'W}{L_{eff}}\left(1+2\frac{W_D}{X_J}\right)^{-\frac{1}{2}}(\phi-V_{BS}+V_{DS})^{-\frac{1}{2}} \\
&\cdot\left[(V_{DSAT}-V_{BS}+\phi)^{\frac{3}{2}}-(\phi-V_{BS})^{\frac{3}{2}}\right]
\end{aligned}
$$

where the derivative of the saturation voltage is described in case 1.

* Case 4: λ not input, V_{MAX} input:

$$
\begin{aligned}
g_o \;=\;& -\frac{\gamma}{4}\cdot\frac{X_D}{L_{adj}}\cdot\frac{UEXP}{V_{GS}-V_{TH}}(\phi-V_{BS})^{\frac{1}{2}}\left(1+2\frac{W_D}{X_J}\right)^{-\frac{1}{2}}(\phi-V_{BS}+V_{DS})^{-\frac{1}{2}}I_{DS} \\
&+\frac{1}{2}\cdot\frac{X_D}{L_{eff}}\left[\left(\frac{X_D V_{MAX}}{2\mu_s}\right)^2+V_{DS}-V_{DSAT}\right]^{-\frac{1}{2}}\left(1-\frac{\partial V_{DSAT}}{\partial V_{DS}}\right)I_{DS} \\
&-\frac{\gamma}{}\cdot\frac{X_D}{}\cdot\frac{UEXP}{}(\phi-V_{BS})^{\frac{1}{2}}\left(1+2\frac{W_D}{}\right)^{-\frac{1}{2}}(\phi-V_{BS}+V_{DS})^{-\frac{1}{2}}
\end{aligned}
$$

$$
\begin{aligned}
&\cdot\left\{\frac{X_D^2 V_{MAX}}{2L_{adj}\mu_s}-\frac{X_D}{L_{adj}}\left(\frac{X_D V_{MAX}}{2\mu_s}\right)^2\left[\left(\frac{X_D V_{MAX}}{2\mu_s}\right)^2+V_{DS}-V_{DSAT}\right]^{-\frac{1}{2}}\right\} I_{DS}\\
+\;&\frac{K_2' W}{L_{eff}}\left[V_{GS}-V_{TH}^{*}-\eta V_{DSAT}-\gamma_s(V_{DSAT}-V_{BS}+\phi)^{\frac{1}{2}}\right]\frac{\partial V_{DSAT}}{\partial V_{DS}}\\
+\;&\frac{\gamma}{6}\cdot\frac{X_D}{L_{adj}}\cdot\frac{K_2' W}{L_{eff}}\left(1+2\frac{W_D}{X_J}\right)^{-\frac{1}{2}}(\phi-V_{BS}+V_{DS})^{-\frac{1}{2}}\\
&\cdot\left[(V_{DSAT}-V_{BS}+\phi)^{\frac{3}{2}}-(\phi-V_{BS})^{\frac{3}{2}}\right]
\end{aligned}
$$

where the saturation voltage and its derivative were introduced in case 2.

For rough calculations, however, the simple approximated models available to the circuit designers neglect the second order effects. Typical and widely used models for hand calculations are

$$I_{DS}=\frac{K'W}{2L}\cdot(V_{GSQ}-V_T)^2$$

$$g_o=\lambda I_{DSQ}$$

The discrepancies between the SPICE Level2 large-signal MOSFET model and the drain current approximation used in hand calculations are shown in fig.1. Considering the case where λ and V_{MAX} are not entered as input parameters, fig.2 illustrates a comparison of the output conductance as predicted by SPICE, as predicted by the exact analytical expression, and as predicted by using SPICE to calculate a numerical derivative approximation of the partial derivative of the drain current. In these plots, g_{oSPICE} is the output conductance implemented in SPICE, g_{oHC} is the output conductance mathematically computed by taking the exact derivative of the drain-to-source current expression, g_{oND} is the output conductance obtained by using SPICE to the numerical difference of the drain current. The simulations leading to the plotted results of fig.1 and fig.2 were run with a minimum-size device and typical process parameters describing a CMOS 2µm fabrication process.

Note that the numerical derivative and the exact analytical expression of g_o are in close agreement but differ significantly from the value of g_o predicted by SPICE. This difference makes the SPICE small signal model non self-consistent with its large-signal counterpart.

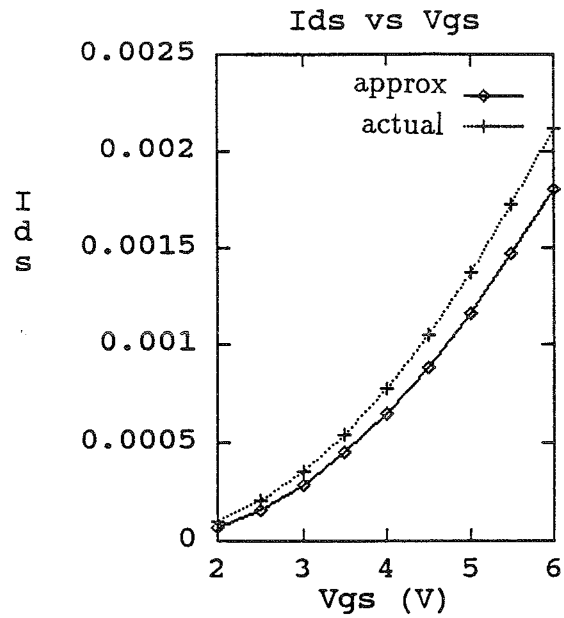

fig.1

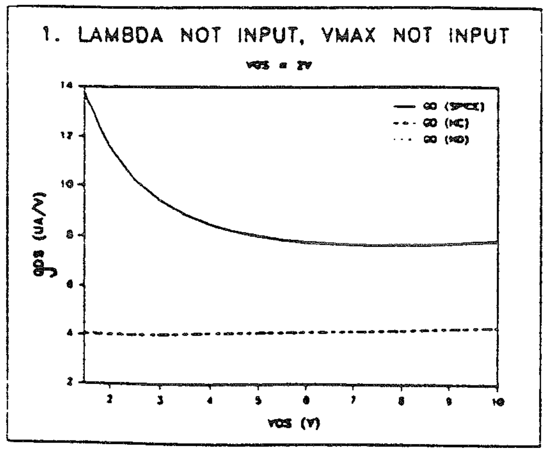

fig.2

III. COMPUTER TOOL DESCRIPTION

The above plots illustrate the discrepancies between computer models and models used for hand calculations. Note that the approximated models are expressed in terms of multivariable polynomials of process variables and terminal electrical variables of the MOSFET device. In order to keep this simplicity in approximated models, a tool has been developed which generates multivariable polynomial expressions for the models describing the MOS transistor. This algorithm is based upon expanding the functions of interest in a truncated multivariable Taylor series by using a forward finite-difference method to approximate the ordinary and mixed partial derivatives of the expansion. For simplycity purposes this section will focus on the expansion of a function of two variables. The Taylor series of a function f of two variables x and y around the point (x_o, y_o) can be expressed as follows:

$$f(x,y) = \sum_{k=0}^{\infty} \frac{1}{k!} \left[(x - x_0)\frac{\partial}{\partial x} + (y - y_0)\frac{\partial}{\partial y} \right]^k f(x,y) \Bigg|_{y=y_0}^{x=x_0}$$

Each partial derivative is being evaluated by computing a forward numerical differentiation scheme using a regular spacial distribution of the points of evaluation. For instance, a forward derivative expression can be developed at $x = x_i$, using a 2^{nd} order polynomial. Assuming the following notation:

$$f_{i+1} = f(x_{i+1}) \quad \text{with} \quad x_{i+1} = x_i + h$$

$$f_{i+2} = f(x_{i+2}) \quad \text{with} \quad x_{i+2} = x_i + 2h$$

the first forward derivative is determined by expanding a Taylor series about the points x_{i+1} and x_{i+2}. Therefore,

$$f_{i+1} = f_i + hf_i^{(1)} + \frac{h^2}{2!} f_i^{(2)} \pm error$$

$$f_{i+2} = f_i + (2h)f_i^{(1)} + \frac{(2h)^2}{2!} f_i^{(2)} \pm error$$

Combining the above equation and solving for $f_i^{(1)}$, the first forward derivative approximation using an order-two polynomial is obtained:

$$f_i^{(1)} = \frac{1}{2h}(-3f_i + 4f_{i+1} - f_{i+2})$$

Where $(O)h^2$ is the order of error associated with the finite diference approximation.
The software implements the approximation of partial ordinary and mixed derivatives up to the 7th order for arbitrary multivariable functions. In order to perform an accurate evaluation of each derivative, the computer tool carries out an automatic procedure for scaling the discretization step h. When the relative difference between two consecutive computations of a given derivative falls below a preassigned small value, the calculation is stopped and it is asumed that an accurate value of the approximated derivative has been found.

IV. EXAMPLES OF APPROXIMATION

The discussion focuses on the approximation of the drain-to-source current with models of dimension one through four.

* <u>One-dimensional approximated model</u>

The expansion of the drain-to-source current up to the 7th order around the quescient value of the gate-to-source voltage (V_{GSQ} = 2.0V) led to the obtention of 8 approximated derivatives. Fig. 3 shows the evaluation of the approximated function for a range of V_{GS} of 4.0 volts. Comparing the approximated value and the actual value of I_{DS}, note that the maximum relative error is 3.0%. For a gate-to-source voltage of 3.0V, the relative error is far less than 1.0% (error = 0.43%).
For V_{GSE} = 3.0V, I_{DS} can be expressed as:

$$I_{DS} = 6.8404E - 05 + 0.14625E - 03(V_{GS} - V_{GSQ})$$
$$+ \ 0.75096E - 04(V_{GS} - V_{GSQ})^2$$

the other coefficients of the expansion being neglected since their overall contribution only reaches 0.02%.

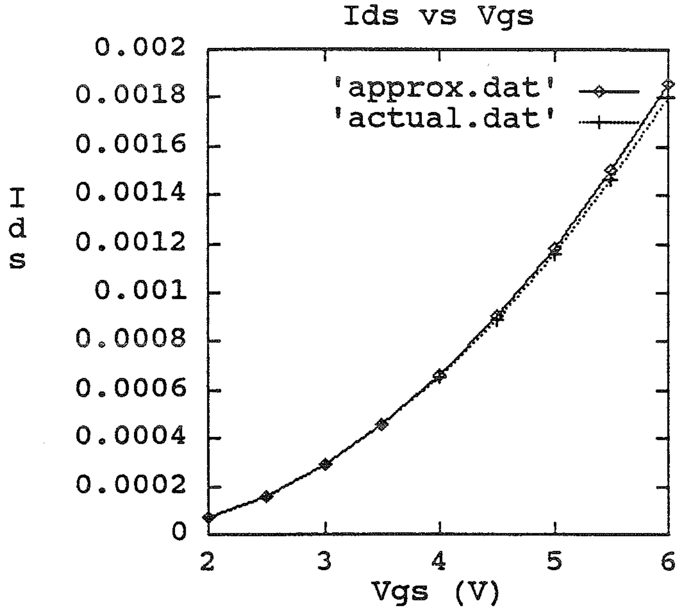

fig.3

* <u>Two-dimensional approximated model</u>

The drain current was expanded with respect to two variables V_{GS} and V_T around their quiescent value. The total number of approximated derivatives computed reached 36. For V_{GSE} = 3.0V, the number of coefficients of the expansion can be reduced to 6 since the total contribution of the other coefficients represents a negligible percentage (0.17%).
I_{DS} is then written as:

$$\begin{aligned} I_{DS} &= 6.8404E-05+0.14625E-03(V_{GS}-V_{GSQ})-0.14625(V_T-V_{TQ}) \\ &+ 0.75088E-04(V_{GS}-V_{GSQ})^2+0.75442E-04(V_T-V_{TQ})^2 \\ &- 0.15038E-03(V_{GS}-V_{GSQ})(V_T-V_{TQ}) \end{aligned}$$

* <u>Four-dimensional approximated model</u>

The expansion was performed with respect to four variables V_{GS}, V_T, V_{DS} and K'. The computer tool determined 307 coefficients for the Taylor series expansion. This very high number can be reduced to 8. The relative error between the approximated evaluation and the actual value of the drain current is then equal to 0.09% at V_{GSE}=3.0V. The approximated expression of I_{DS} can therefore simply represented by the following summation of 8 terms.

$$\begin{aligned} I_{DS} &= 6.8404E-05 + 0.14625E-03(V_{GS}-V_{GSQ}) - 0.14625(V_T - V_{TQ}) \\ &+ 0.23487E-05(V_{DS}-V_{DSQ}) + 0.75091E-04(V_{GS}-V_{GSQ})^2 \\ &+ 0.75442E-04(V_T-V_{TQ})^2 + 0.37114E-05(V_{GS}-V_{GSQ})(V_{DS}-V_{DSQ}) \\ &- 0.15036E-03(V_{GS}-V_{GSQ})(V_T-V_{TQ}) \end{aligned}$$

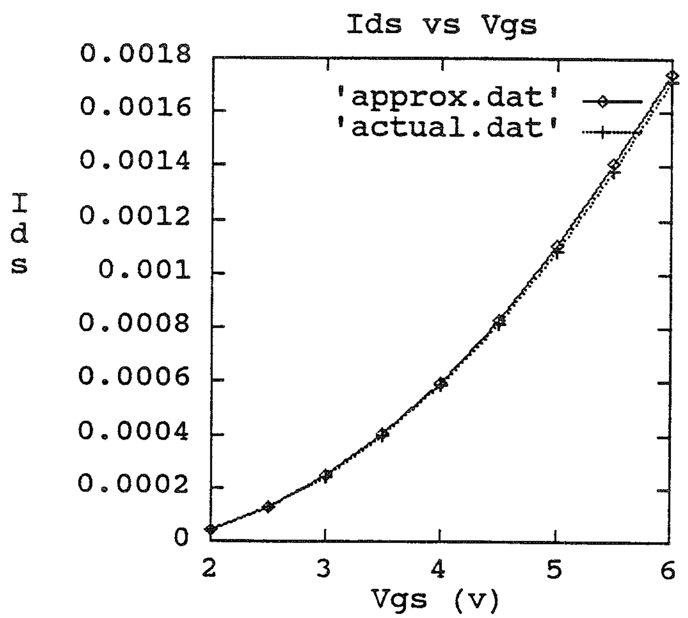

fig.5

All simulations were run for V_{GSQ}=2.0 V, V_{TQ}=0.93 V, V_{DSQ}=6.0 V.

V. CONCLUSIONS

In this paper, a computer tool for generation of simple, mathematically tractable and accurate models for electronic devices was introduced. Simulations of a MOS drain current showed a very good agreement between the approximated expression and the exact closed-form equation (less than 1.0% error) and consequently allowing the rewriting of the drain current expression in terms of a multivariable polynomial with very few terms. However, when the order of the expansion exceeds 4, some problems were encoutered which prevented an expansion involving more variables and higher order terms. The time consumption becomes critical at higher order expansions and the step size algorithm needs some fine adjustments. The next application should be the development of new models of the much needed small-signal output conductance of the MOS transistor.